INTERFEROMETRIC CHARACTERIZATION OF AREAS DAMAGED BY THE 1995 KOBE EARTHQUAKE USING SATELLITE SAR IMAGES

Masashi MATSUOKA[1] And Fumio YAMAZAKI[2]

SUMMARY

The coherence analysis of synthetic aperture radar (SAR) onboard a satellite was applied to detect earthquake damage distribution. We investigated the microwave scattering characteristics of areas damaged by the 1995 Kobe earthquake using satellite JERS-1/SAR images whose swath width and spatial resolution are approximately 100km and 30m, respectively. According to the difference in backscattered intensity and coherence from interferometric analysis of SAR images taken at different times, we found that the characteristics of backscattering property of damaged areas showed significant variations. Therefore, the images obtained by remote sensing SAR can be a powerful tool for post-disaster management. Finally, we introduce a recent airborne SAR system which provides 1.5m high-resolution images based on interferometry and full-polarimetry and present an example.

INTRODUCTION

To gather information on damage carried by natural disasters, several methods exist, such as field surveys, aerial videography and photography, and satellite imagery. Satellite remote sensing, by means of which a large area can be easily monitored, may provide effective information at the time of recovery activities such as devising a restoration plan, if it is possible to determine the distribution of damage at an early stage. Several satellites observed the Kobe area [Sudo *et al.*, 1995] before and after the Hyogoken-Nanbu (Kobe) earthquake, which occurred on January 17, 1995. Multispectral characteristics differed between images of liquefied areas and burned areas taken by airborne remote sensing just after the earthquake occurred [Mitomi and Takeuchi, 1995]. A study suggested the possibility of interpreting the damaged area based on the spectral pattern changes between optical satellite images taken before and after this earthquake [Inanaga *et al.*, 1995]. Some authors have already reported spectral characteristics of the damaged area performing this type of comparison with the detailed damage survey results of this earthquake, and have attempted to identify the damage distribution from satellites, Landsat and SPOT, optical images [Matsuoka and Yamazaki, 1998].

Synthetic aperture radar (SAR) observations can be performed night and day and are not influenced by the weather conditions. This feature could be useful for effective postdisaster assessment when optical remote sensing, such as multispectral scanning and aerial photography or a field survey for a large area is difficult. Earth observation satellites equipped with SAR, containing information on the amplitude and phase of microwave backscattering from objects on the earth's surface, observed the areas hit by recent big earthquakes. Massonnet *et al.* (1993) introduced SAR interferometric analysis using phase information to estimate the distribution of ground displacement due to the 1992 Landars earthquake and Ozawa *et al.* (1997) applied the same technique for the Kobe earthquake. For building damaged area estimation, studies on interpreting distribution of damage due to the Kobe earthquake were reported using ERS/SAR amplitude information [Aoki *et al.*, 1998; Yonezawa and Takeuchi, 1998a] and phase information [Yonezawa and Takeuchi, 1998b]. Aoki *et al.* (1998) reported that the estimated damage distribution based on the relationship between the building damage ratio and SAR intensity images taken in the pre- and post-earthquake periods showed relativery good agreement with the actrual damage belt. However, because the post-event image was taken 4 months after the earthquake, a

[1] *Chief Research Engineer, Earthquake Disaster Mitigation Research Center, RIKEN, Japan, Email: matsuoka@miki.riken.go.jp*
[2] *Team Leader, Earthquake Disaster Mitigation Research Center, RIKEN, Japan, Email: yamazaki@iis.u-tokyo.ac.jp*

direct comparison between the images and damaged areas was not accurate. Japanese satellite JERS observed the Kobe area 20 days after the event. Matsuoka and Yamazaki (1999) tried to identify the damage distribution using JERS/SAR intensity images. However the result from JERS/SAR was not so good compared with that from ERS/SAR. Another approach to use the phase information, which is more sensitive than the intensity value, revealed a good relationship between the damaged area and phase information using JERS/SAR images [Rosen *et al.*, 1999].

Applications of SAR interferometry to identify the building damaged areas were attempted by several researchers, but no quantitative approach was found for examining the backscattering properties of the damaged area based on detailed damage survey results. Since a part of the damage survey results of the Kobe earthquake was maintained as GIS data, a quantitative analysis of the superficial changes in the damaged area was possible. In this study, the amplitude and coherency of backscattered echoes of the damaged areas were investigated using JERS/SAR images taken before and after the earthquake.

DATASET

SAR Images

We used the JERS/SAR image observed on February 5, 1995, 20 days after the Kobe Earthquake, and also used pre-event images taken on September 8, 1992, October 22,1992, May 30,1993, November 22,1993 and February 18,1994 to examine the change in the backscattering characteristics of the damaged area. The main characteristics of JERS/SAR systems are listed in Table 1. SAR systems have the capability of recording complex signals including the amplitude (intensity) and phase of backscattered echoes from objects on the earth's surface. We obtained complex signals using processing software from SAR Level 0 signal data [Ono and Yamanokuchi, 1997]. Backscattered intensity image taken after the earthquake and the area covered by the satellite image is shown in Fig. 1 and Fig. 2, respectively.

Table 1: Characteristics of JERS/SAR

Frequency	1.275GHz (L-band)
Wavelength	23.5 cm
Polarization	HH
Incidence Angle	38.7°
Swath Width	75 km
Spatial Resolution	18 m
Recurrence Period	44 days

Earthquake Damage Survey

Building damage was focused on as a form of earthquake damage in this study. The building damage data based on detailed survey results compiled by AIJ (the Architectural Institute of Japan) and CPIJ (the City Planning Institute of Japan), and digitized by BRI (Building Research Institute, Ministry of Construction) were utilized as GIS data. In the GIS data, the building damage level was classified into five categories: damage by fire, severe damage, moderate damage, slight damage and no damage, and the numbers of damaged buildings were totaled for each block in each ward [Building Research Institute, 1996]. The area of the damage survey data and the hard-hit zone calculated from this data are also shown in Fig. 1.

Registration and Geometric Correction of SAR Images

We overlaid the sets of two SAR images and calculated the complex coherence, which is described in the next section, for the area of the 7 x 7 pixel window around the initial position. Then matched positions were shifted, pixel by pixel, within the 15 x 15 pixel window to find the position at which the two images match best. By this procedure, the optimum pixel pair was determined at the position that yields the highest coherence and used to match all SAR images using the bilinear transformation. The pixel pairs were also used as ground control point (GCP) for the affine geometric correction to overlay SAR images with the damage survey data.

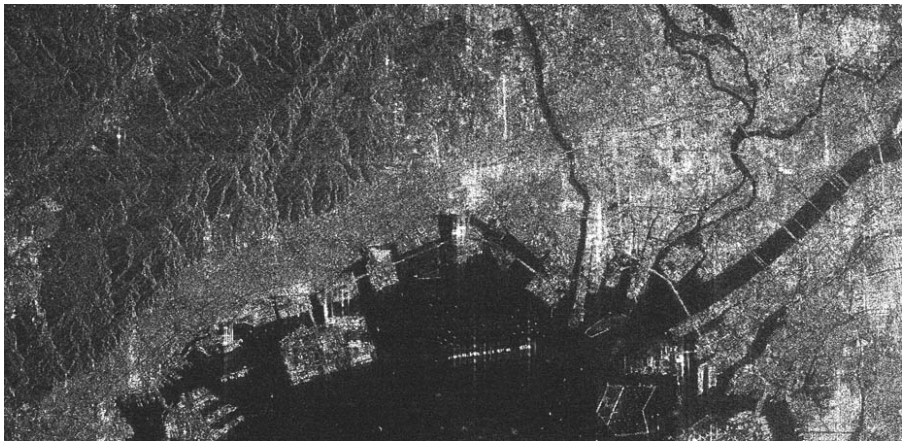

Figure 1: Backscattered intensity image of JERS/SAR taken after the Kobe earthquake (February 5, 1995)

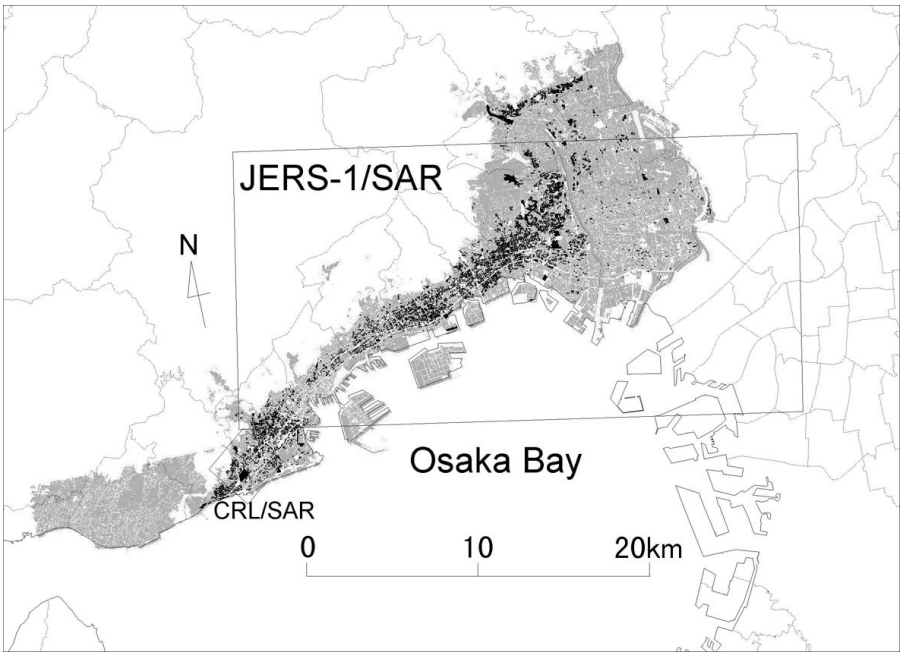

Figure 2: Area of this study. Large and small rectangles indicate the areas of JERS/SAR and airborne SAR, respectively. Black area indicates the distribution of hard-hit areas based on building damage data by BRI (1996).

INTERFEROMETRIC ANALYSIS

The coherence, which is the correlation calculated with the phase of the backscattering echo of two co-registered complex SAR images, is a suitable and sensitive parameter for change detection and land use classification. The complex coherence γ of two complex signals z_1 and z_2 is defined in equation (1), given N signal measurements,

$$\gamma = \frac{\sum_{i=1}^{N} z_{1i} z_{2i}^{*}}{\sqrt{\sum_{i=1}^{N} |z_{1i}|^2} \sqrt{\sum_{i=1}^{N} |z_{2i}|^2}} \quad , \tag{1}$$

where i is the sample number. This approach is usually adopted between two co-registered complex images acquired under slightly different geometrical configurations; however, decorrelated areas exist in the coherence image. The main sources of decorrelation include spatial or temporal decorrelation. The spatial decorrelation is derived from the difference in the geometry of observation between two acquisitions, which is called baseline length B, as shown in Fig. 3. The temporal decorrelation is related to an atmospheric effect such as moisture and/or surface changes within two acquisitions.

The time intervals and the baseline between two observations in our dataset are listed in Table 2. Four pairs were selected to calculate the degree of coherence and N is defined as 81 pixels in this study. Two pairs, pair-A1 and A2, are used as the pre- and post-event images. Pair-A1 was a pair of Sep. 8, 1992 and Feb. 5,1995 with short baseline, pair-A2 was a pair of Feb. 18, 1994 and Feb. 5, 1995 with a relatively short time interval. Pairs-B1 and B2, of Oct. 22,1992 and Nov. 22,1993, May 30,1993 and Feb. 18,1994 were called pair-B1 and B2, respectively, were prepared using pre- and pre-event images to examine the variation of coherence in the urban area within the usual acquisition time.

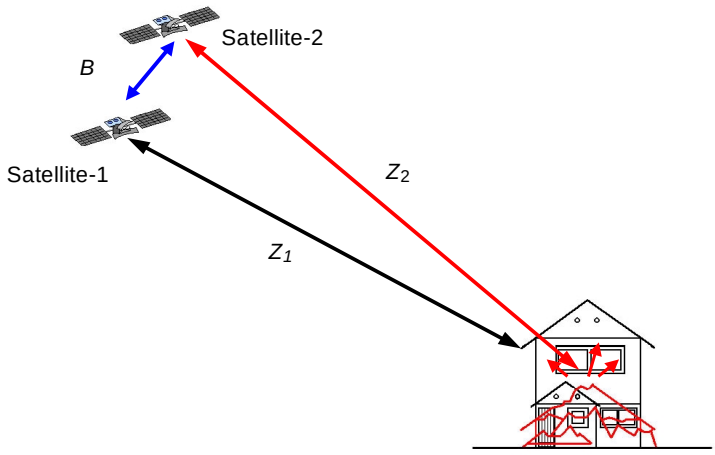

Figure 3: Basic principle of the repeat pass radar interferometry

Table 2: Time intervals and baselines

Time interval [days] (top) and baseline [km] (bottom) as estimated from orbit data
1) pair-A1, 2) pair-A2, 3) pair-B1, 4) pair-B2

	92/09/08	92/10/22	93/05/30	93/11/22	94/02/18	95/02/05
92/09/08		44 4623	264 6166	440 5052	528 6134	880 [1] 344
92/10/22			220 1533	396 [3] 542	484 1572	836 4899
93/05/30				176 1096	264 [4] 245	616 6398
93/11/22					66 1088	440 5340
94/02/18						352 [2] 6423
95/02/05						

CHARACTERISTICS OF SAR IMAGES

The pixels that represent the areas of burning, heavy damage, slight damage and no damage of buildings were selected from the SAR images in order to examine the characteristics of the intensity and coherence in the earthquake damaged area. The pixels for the burned class were selected from the city blocks where all buildings burnt down. Pixels were also selected from the city blocks where all buildings were determined to have severe or moderate structural damage and slight damage, and categorized into heavy and slight damage classes, respectively. We selected pixels in nondamaged areas for the nondamaged class. The 500 pixels for each class of damage were selected to analyze. Although there is a slight influence of vegetation even in the SAR images, we disregarded it in this analysis.

Table 3: Average value of backscattered intensity of SAR images for the classified damaged areas before and after the earthquake

Classified damaged area	Number of pixels	Intensity [dB] : average (s.d.)	
		1995/02/05	1993/05/30
Burned	500	37.9 (6.1)	34.0 (6.2)
Heavy Damage	500	38.8 (6.4)	34.0 (6.2)
Slight Damage	500	39.4 (6.8)	33.7 (6.2)
No Damage	500	39.5 (6.8)	33.5 (7.1)

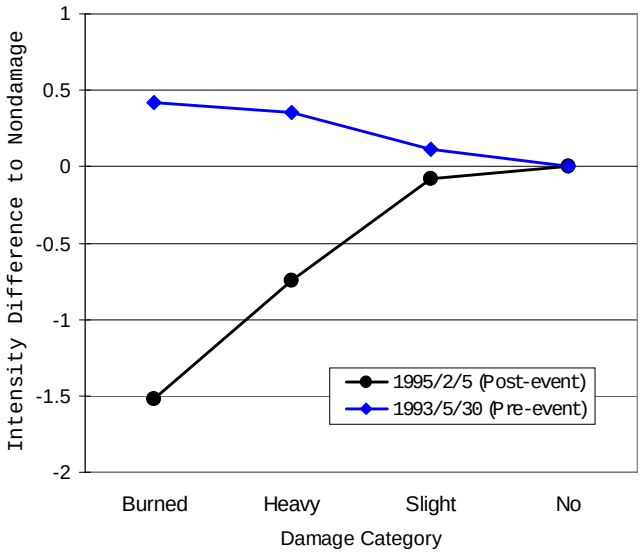

Figure 4: Defference in backscattered intensity between damaged and nondamaged areas before and after the earthquake

The characteristics of the mean value and the standard deviation of backscattered intensity in each area classified as damaged by the earthquake are shown in Table. 3. These values in the pre-event image taken on May 30,1993 are also shown in Table 3. The trends of the values of intensity difference to the nondamaged area are shown in Fig. 4. Table 3 and Figure 4 show that the intensity values of the severely damaged area in post-event image are smaller than those of the nondamaged area, although the standard deviations are quite large. However, a similar trend is not observed in the pre-event image. Generally, buildings show comparatively high reflectance because of the specular characteristics of the structure and the ground surface. Open spaces or damaged buildings have low reflectance because the microwaves are scattered in different directions. Following the earthquake, buildings were destroyed and in some cases the debris cleared leaving the ground exposed. Therefore, it is

considered that the intensity determined in damaged areas is lower in comparison with than that in nondamaged areas.

The mean and standard deviation of the magnitude of complex coherence $|\gamma|$ for each damage class for the four pairs are shown in Table 4. Figure 5(a) shows the behavior of mean values. Especially in pair-A1, we found the trend in the area of a higher damage class was revealed when the coherency became low. This result is considered to depend on the influence of superficial changes due to building collapse. Although not so obvious, a similar trend is observed in pair-A2. Theoretically, the coherence and the sensitivity of coherency become low under the condition of a long baseline. Generally, because superficial changes may occur during a long time interval between two acquisitions, the coherence becomes low. The relationship between the coherence of nondamaged areas and the value of the baseline length times the time interval is shown in Fig. 5(b). As the value increases the coherence becomes low, which agree with recent studies. It is considered that the long baseline brought about the decorrelation and low sensitivity of pair-A2 in spite of a short time interval.

Table 4: Average value of coherence of SAR images for the classified damaged areas

Classified damaged area	Number of pixels	Coherence: average (s.d.)			
		Pair-A1	Pair-A2	Pair-B1	Pair-B2
Burned	500	0.19 (0.09)	0.18 (0.10)	0.26 (0.14)	0.29 (0.15)
Heavy Damage	500	0.21 (0.12)	0.20 (0.12)	0.27 (0.14)	0.28 (0.15)
Slight Damage	500	0.25 (0.14)	0.23 (0.13)	0.30 (0.16)	0.37 (0.17)
No Damage	500	0.28 (0.15)	0.23 (0.13)	0.29 (0.15)	0.35 (0.18)

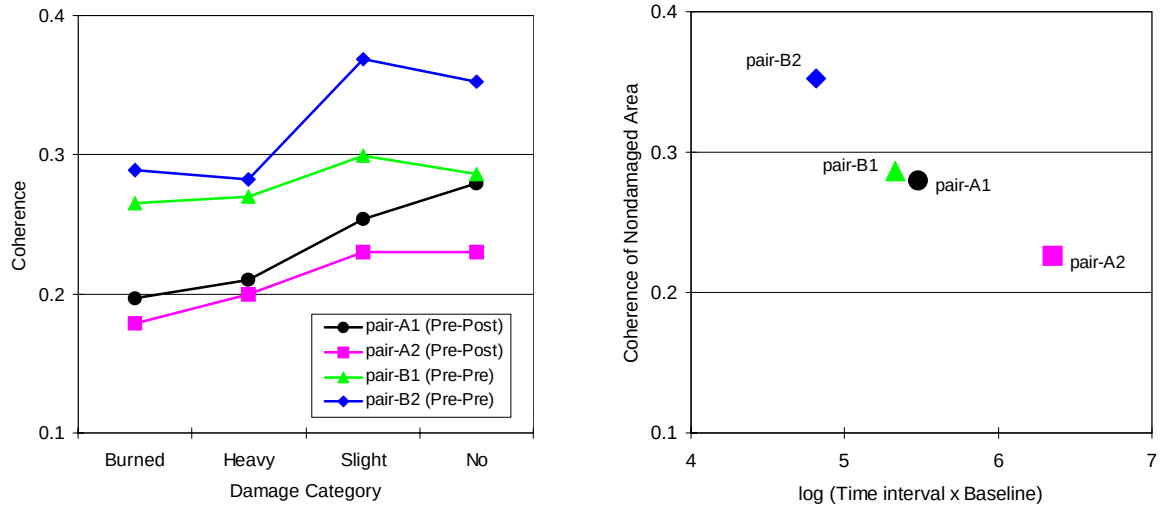

(a) **(b)**

Figure 5: Degree of coherence of each pair for damage classes (a); and relationship between coherence and value of time intervals times baseline (b)

From the pair of pre-event images, we observed small differences of coherence in each damage class in pair-B1. However, there is quite a large variation in pair-B2 with a very short baseline. We currently lack definite information on this result and further investigation will be necessary to identify the coherency in an urban area. However the degree of coherence shows that it is possible to capture changes such as building collapse from SAR images in spite of a large standard deviation existing in the damage classification categories.

AIRBORNE SAR

Recently, an airborne SAR observation system as shown in Fig. 6(a), as developed by the Communications Research Laboratory (CRL), the Ministry of Posts and Telecommunications and the National Space Development Agency of Japan (NASDA). Airborne SAR images taken by multifrequency, X- and L-band, and full-polarimetric (HH, VV, HV, VH) observation contain useful quantitative values for detecting objects with high ground resolution, 1.5m and 3m for X- and L-band, respectively.

Figure 6(b) shows an example of a SAR backscattered intensity image of the Nagata area in Kobe. Many buildings are clearly seen because of their strong microwave reflection tendencies. Tall buildings are displayed with three-dimensional characteristics, which are easily distinguishable. In order to utilize this system for prompt and accurate monitoring of natural disasters, we plan to evaluate the relationship between surface deformation, such as is due to earthquakes and typhoons and the reconstruction after these disasters and backscattering properties using several SAR images taken at different acquisitions.

(a)

(b)

Figure 6: Aircraft equipped with SAR system (a); and image of Nagata area, Kobe (b) [CRL and NASDA, 1998]

CONCLUSIONS

This paper reported on quantitative evaluation about the backscattering properties, such as intensity and coherence of areas damaged by the 1995 Kobe earthquake using synthetic aperture radar (SAR) images from satellite JERS, to examine the possibility of capturing earthquake damage distribution. The relationship between building damage and the SAR images was found to be related to the damage level. This trend in areas of heavy building damage was revealed when the backscattered intensity and the coherence of pre- and post-event images became low. In spite of these results regarding the mean characteristics of satellite images, a large degree of randomness still exists in each damage classification category. Hence, further study will be necessary using a recently developed airborne SAR system with very high resolution for earthquake damage survey in urban areas.

ACKNOWLEDGMENTS

We thank Mr. Ronald T. Eguchi of EQE International, Inc. for his helpful advice on detecting earthquake damage of man-made structures using the interferometric approach. The JERS images used in this study are owned by the Ministry of International Trade and Industry (MITI) and National Space Development Agency of

Japan (NASDA). JERS/SAR image processing was conducted using programs coded by Mr. Makoto Ono of the Remote Sensing Technology Center of Japan. Airborne SAR images were used in the cooperative research with Communications Research Laboratory (CRL), Ministry of Posts and Telecommunications.

REFERENCES

Aoki, H., Matsuoka, M. and Yamazaki, F. (1998), "Characteristics of Satellite SAR Images in the Damaged Areas due to the Hyogoken-Nanbu Earthquake", *19th Asian Conf. of Remote Sensing*, pp.C7/1-6.

Building Research Institute (1996), *Final Report of Damage Survey of the 1995 Hyogoken-Nanbu Earthquake* (in Japanese).

Communication Research Laboratory, Ministry of Posts and Telecommunications and National Space Development Agency of Japan (1998), *CRL/NASDA Airborne Synthetic Aperture Radar*.

Inanaga, A., Tanaka, S., Takeuchi, S., Takasaki, K. and Suga, Y. (1995), "Remote Sensing Data for Investigation of Earthquake Disaster", *21st Annual Conf. of the Remote Sensing Society*, pp.1089-1096.

Massonnet, D., Rossi, M., Carmona, C., Adragna, F., Peltzer, G., Fiegl, K. and Rabaute, T. (1993), "The Displacement Field of the Landars Earthquake Mapped by Radar Interferometry", *Nature*, 364, pp.138-142.

Matsuoka, M. and Yamazaki, F. (1998), "Identification of Damaged Areas due to the 1995 Hyogoken-Nanbu Earthquake Using Satellite Optical Images", *19th Asian Conf. of Remote Sensing*, pp.Q9/1-6.

Matsuoka, M. and Yamazaki, F. (1999), "Characteristics of Satellite Images of Damaged Areas due to the 1995 Kobe Earthquake", *2nd Conf. on the Applications of Remote Sensing and GIS for Disaster Management*, The George Washington University, CD-ROM.

Mitomi, Y. and Takeuchi, S. (1995), "Analysis of Spectral Feature of the Damaged Areas by Liquefaction and Fire Using Airborne MSS Data", *18th Japanese Conf. on Remote Sensing*, pp.117-118 (in Japanese).

Ono, M. and Yamanokuchi, T. (1997), "Image Reconstruction of JERS-1 SAR Data with PC or EWS", *Earth, Planet and Space Joint Meeting*, p.298 (in Japanese).

Ozawa, S., Murakami, M., Fujiwara, S. and Tobita, M. (1997), "Synthetic Aperture Radar Interferogram of the 1995 Kobe Earthquake and Its Geodetic Inversion", *Geophysical Research Letters*, Vol.24, No.18, pp.2327-2330.

Rosen, P. A., Hensley, S., Peltzer, G. Rignot, E. and Werner, C. (1999), "JERS-1 Synthetic Aperture Radar Interferometry Applications, - Mapping of Rain Forest Environment and Crustal Deformation Studies", *JERS-1 Science Program '99 PI Reports, Global Forest Monitoring and SAR Interferometry*, Earth Observation Research Center, NASDA, pp.179-184

Sudo, N., Tada, T., Nakano, R., Cho, K., Shimoda, H. and Sakata, T. (1995), "Multi-Stage Remote Sensing on the Great Hanshin Earthquake Disaster Survey", *18th Japanese Conf. on Remote Sensing*, pp.115-116 (in Japanese).

Yonezawa, C. and Takeuchi, S. (1998a), "Detection of Damaged Built-up Areas by the 1995 Hyogoken-Nanbu Earthquake Using ERS-1/SAR Intensity Images", *Photogrammetric Engineering and Remote Sensing*, Vol. 37, No. 4, pp.57-61 (in Japanese).

Yonezawa, C. and Takeuchi, S. (1998b), "Change Detection of Backscattering Characteristics on the Ground in SAR Imagery - Comparison between Intensity and Coherence -", *24th Japanese Conf. On Remote Sensing*, pp.119-120 (in Japanese).